Inorg. Chem. **2008**, *47*, 9716−9722

Novel Heterometallic Fe−Ru_2−Fe Arrays via "Complex of Complexes" Approach

Cai-Feng Wang,[†] Jing Lin Zuo,*[,†] Jie-Wen Ying,[‡] Tong Ren,*[,‡] and Xiao-Zeng You[†]

State Key Laboratory of Coordination Chemistry, School of Chemistry and Chemical Engineering, Nanjing University, Nanjing 210093, P. R. China, Department of Chemistry, Purdue University, West Lafayette, Indiana 47907

Received June 24, 2008

Four tetranuclear heterometallic compounds, $[(Tp)Fe(CN)_3]_2[Ru_2(DMBA)_4]$ (**1**), $[(MeTp)Fe(CN)_3]_2[Ru_2(DMBA)_4]$ (**2**), $[(^tBuTp)Fe(CN)_3]_2[Ru_2(DMBA)_4]$ (**3**), and $[(PhTp)Fe(CN)_3]_2[Ru_2(DMBA)_4]$ (**4**) [DMBA = *N,N′*-dimethylbenzamidinate, Tp = (hydrotris(pyrazolyl)borate, MeTp = (methyltris(pyrazolyl)borate, ^{t}BuTp = (2-methylpropyltris(pyrazolyl)borate, and PhTp = (tris(pyrazolyl)phenylborate)] were prepared from the combination of $Ru_2(DMBA)_4(NO_3)_2$ and an appropriate $[(RTp)Fe(CN)_3]^-$. Molecular structures of compounds **1**−**4** were established using single-crystal X-ray diffraction, and all feature a linear Fe−C≡N−Ru−Ru−N≡C−Fe array. The magnetic study revealed that the temperature dependence of $\chi_M T$ is mostly attributed to the zero-field splitting of the Ru_2 center, indicating the absence of strong spin coupling among three metallic centers. The electronic independence was further confirmed by the vis−NIR spectroscopic studies. Also described are the voltammetric properties of these compounds.

Introduction

Linear arrays of conjugated molecules, both organic and inorganic, are both fundamentally interesting and technologically important because of the intricate electronic structures that exist in these arrays and the potential of realizing molecular photonic and electronic wires based on the arrays.[1−6] Unique among these molecular arrays are the species containing metal−metal bonds in the backbones, whereas molecular wire behaviors and novel optical and magnetic characteristics have been uncovered.[7−12] Diruthenium compounds in particular have attracted intense interest because of their rich redox, magnetic, sensory, and optical properties[5,13−20] and recently demonstrated molecular wire and switch characteristics.[21,22]

Assembly of diruthenium arrays may be achieved through the linkage at either the axial[23,24] or the equatorial posi-

* Authors to whom correspondence should be addressed. E-mail: zuojl@nju.edu.cn (J.L.Z.) and tren@purdue.edu (T.R.).
† Nanjing University.
‡ Purdue University.

(1) Martin, R. E.; Diederich, F. *Angew. Chem., Int. Ed.* **1999**, *38*, 1350.
(2) Schwab, P. F. H.; Levin, M. D.; Michl, J. *Chem. Rev.* **1999**, *99*, 1863.
(3) Paul, F.; Lapinte, C. *Coord. Chem. Rev.* **1998**, *178*−*180*, 431.
(4) Low, P. J. *Dalton Trans.* **2005**, 2821.
(5) Ren, T. *Organometallics* **2005**, *24*, 4854.
(6) Paul, F.; Lapinte, C. In *Unusual Structures and Physical Properties in Organometallic Chemistry*; Gielen, M., Willem, R., Wrackmeyer, B., Eds.; Wiley: West Sussex, U.K., 2002.
(7) Cotton, F. A.; Murillo, C. A.; Walton, R. A. *Multiple Bonds between Metal Atoms*; Springer Science and Business Media, Inc.: New York, 2005.
(8) Chae, D.-H.; Berry, J. F.; Jung, S.; Cotton, F. A.; Murillo, C. A.; Yao, Z. *Nano Lett.* **2006**, *6*, 165.
(9) Yeh, C.-Y.; Wang, C.-C.; Chen, C.-H.; Peng, S.-M. In *Redox Systems under Nano-Space Control*; Hirao, T., Ed.; Springer: Berlin, 2006.
(10) Chen, I.-W. P.; Fu, M.-D.; Tseng, W.-H.; Yu, J.-Y.; Wu, S.-H.; Ku, C.-J.; Chen, C.-h.; Peng, S.-M. *Angew. Chem., Int. Ed.* **2006**, *45*, 5814.
(11) Chisholm, M. H.; Macintosh, A. M. *Chem. Rev.* **2005**, *105*, 2949.
(12) Chisholm, M. H. *Proc. Natl. Acad. Sci. U.S.A.* **2007**, *104*, 2563.
(13) Zuo, J.-L.; Herdtweck, E.; Kühn, F. E. *Dalton Trans.* **2002**, 1244.
(14) Chen, L.; Ramsey, C. M.; Dalal, N. S.; Ren, T.; Cotton, F. A.; Wernsdorfer, W.; Chiorescu, I. *Appl. Phys. Lett.* **2006**, *89*, No. 252502.
(15) Xu, G.-L.; Wang, C.-Y.; Ni, Y.-H.; Goodson, T. G.; Ren, T. *Organometallics* **2005**, *24*, 3247.
(16) Nakanishi, T.; Ariga, K.; Thuriere, A.; Bear, J. L.; Kadish, K. M. *Thin Solid Films* **2006**, *499*, 349.
(17) Kadish, K. M.; Nguyen, M.; Caemelbecke, E. V.; Bear, J. L. *Inorg. Chem.* **2006**, *45*, 5996.
(18) Han, B.; Shao, J.; Ou, Z.; Phan, T. D.; Shen, J.; Bear, J. L.; Kadish, K. M. *Inorg. Chem.* **2004**, *43*, 7741.
(19) Kadish, K. M.; Phan, T. D.; Giribabu, L.; Shao, J.; Wang, L.-L.; Thuriere, A.; Caemelbecke, E. V.; Bear, J. L. *Inorg. Chem.* **2004**, *43*, 1012.
(20) Bear, J. L.; Han, B.; Huang, S.; Kadish, K. M. *Inorg. Chem.* **1996**, *35*, 3012.
(21) Blum, A. S.; Ren, T.; Parish, D. A.; Trammell, S. A.; Moore, M. H.; Kushmerick, J. G.; Xu, G.-L.; Deschamps, J. R.; Pollack, S. K.; Shashidhar, R. *J. Am. Chem. Soc.* **2005**, *127*, 10010.
(22) Mahapatro, A. K.; Ying, J.-W.; Ren, T.; Janes, D. B. *Nano Lett* **2008**, 8. in press.
(23) Cotton, F. A.; Kim, Y. M.; Ren, T. *Inorg. Chem.* **1992**, *31*, 2723.
(24) Cukiernik, F. D.; Giroud-Godquin, A.; Maldivi, P.; Marchon, J. *Inorg. Chim. Acta* **1994**, *215*, 203.

10.1021/ic8011684 CCC: $40.75
Published on Web 09/24/2008

Scheme 1. Fe−Ru$_2$−Fe Heterometallics **1**−**4**

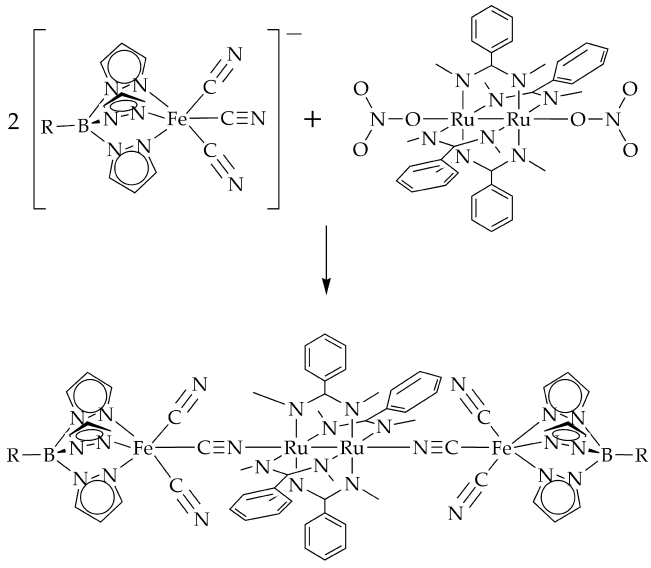

R= H (**1**), Me (**2**), *i*-Bu (**3**) and Ph (**4**)

tions.[25,26] While the use of organic linkers is predominant, two- and three-dimensional arrays of $Ru_2(O_2CR)_4$ have been achieved with $M(CN)_6$-type bridges.[27−30] Use of metal complexes as the bridging unit may result in the "complex of complexes" type of arrays that exhibit rich architectural variety and novel electronic properties from the intermetallic interactions. Recent studies of tricyano-Fe(III) fragments modified with organic ligands revealed their ability as spin centers and interesting magnetic behaviors that include single chain magnets and spin glasses.[31−39] Described in this contribution are the preparation and structural characterization of four *trans*-$[LFe(CN)_3]_2[Ru_2(DMBA)_4]$-type compounds from $Ru_2(DMBA)_4(NO_3)_2$ and $[LFe(CN)_3]^-$ (Scheme 1), where DMBA is *N*,*N*′-dimethylbenzamidinate and L = hydrotris(pyrazolyl)borate (Tp, **1**), methyltris(pyrazolyl)borate (MeTp, **2**), 2-methylpropyltris(pyrazolyl)borate (*i*BuTp, **3**), and tris(pyrazolyl)phenylborate (PhTp, **4**). Also described are the electrochemical, magnetic, and optical properties of compounds **1**−**4**.

Experimental Section

Materials and Measurements. $(Bu_4N)[(Tp)Fe(CN)_3]$, $(Bu_4N)[(MeTp)Fe(CN)_3]$, $(Bu_4N)[(^iBuTp)Fe(CN)_3]$, $(Bu_4N)[(PhTp)Fe(CN)_3]\cdot H_2O$ (Bu_4N^+ = tetrabutylammonium cation), and $Ru_2(DMBA)_4(NO_3)_2$ were synthesized according to the literature methods.[40−42] Spectral pure dichloromethane for electrochemistry and UV−vis spectra measurements were obtained from Aldrich and used without further purification. All other chemicals and solvents were commercially available, analytical reagent-grade, and used as received. Elemental analyses for C, H, and N were performed on a CHN-O-Rapid analyzer and an Elementar Vario MICRO analyzer. Infrared spectra were recorded on a Vector22 Bruker spectrophotometer with KBr pellets in the 400−4000 cm^{-1} region. Vis−NIR absorption spectra were recorded on a Shimadzu UV-3100 spectrometer in CH_2Cl_2 solution. Magnetic susceptibility measurements for all crystalline samples were obtained with the use of a Quantum Design MPMS-XL7 SQUID magnetometer at a temperature range of 1.8−300 K. The dc measurements were conducted with field up to 7 T. Cyclic voltammetry measurements were carried out in CH_2Cl_2 solution at room temperature with a ZAHNER IM6ex electrochemical working station with a glassy carbon working electrode, a platinum wire auxiliary electrode, and a Ag/Ag^+ (10 mM $AgNO_3$ in acetonitrile) reference electrode. The concentration of the complexes was always 1.0 mM, and that of tetrabutylammonium perchlorate was 0.20 M. The ferrocene/ferrocenium (Fc/Fc^+) couple was observed at 0.120 V under the stated conditions.

Caution! *While no problems were encountered in this work, cyanides are very toxic and should be handled in small quantities and with great caution.*

$[(Tp)Fe(CN)_3]_2[Ru_2(DMBA)_4]$ (1). A mixture of methanol and water (v/v 4:1, 12 mL) was gently layered on top of a solution of $Ru_2(DMBA)_4(NO_3)_2$ (18 mg, 0.020 mmol) in 2 mL of acetonitrile and water (v/v 1:1); then, a solution of $(Bu_4N)[(Tp)Fe(CN)_3]$ (24 mg, 0.040 mmol) in 2 mL of methanol was added carefully as a third layer. Dark green needlelike crystals of **1** were obtained after one month. Yield: 60%. Anal. calcd for $C_{60}H_{70}B_2Fe_2N_{26}O_3Ru_2$ (%): C, 46.83; H, 4.58; N, 23.67. Found: C, 46.47; H, 4.63; N, 23.52. IR (KBr, cm^{-1}): 2127 (ν_{CN}).

$[(MeTp)Fe(CN)_3]_2[Ru_2(DMBA)_4]$ (2). A solution of $Ru_2(DMBA)_4(NO_3)_2$ (18 mg, 0.020 mmol) in 8 mL of acetonitrile was added to a solution of $(Bu_4N)[(MeTp)Fe(CN)_3]$ (24 mg, 0.040 mmol) in 4 mL of acetonitrile. To the resultant solution was added 3 mL of isopropanol, which was filtered and left to stand at room temperature. Dark green platelike crystals were obtained after two weeks. Yield: 52%. Anal. calcd for $C_{68}H_{89}B_2Fe_2N_{29}O_6Ru_2$ (%): C, 46.83; H, 5.14; N, 23.29. Found: C, 47.02; H, 4.93; N, 23.17. IR (KBr, cm^{-1}): 2124 (ν_{CN}).

$[(^iBuTp)Fe(CN)_3]_2[Ru_2(DMBA)_4]$ (3). $Ru_2(DMBA)_4(NO_3)_2$ (18 mg, 0.020 mmol) in a mixture of acetonitrile and water (v/v 5:1, 12 mL) was added to a solution of $(Bu_4N)[(^iBuTp)Fe(CN)_3]$ (26 mg, 0.040 mmol) in 3 mL of acetonitrile. Slow evaporation of the resultant solution in the air afforded dark green crystals after two

(25) Angaridis, P.; Berry, J. F.; Cotton, F. A.; Murillo, C. A.; Wang, X. *J. Am. Chem. Soc.* **2003**, *125*, 10327.
(26) Chen, W.-Z.; Ren, T. *Inorg. Chem.* **2006**, *45*, 9175.
(27) Yoshioka, D.; Mikuriya, M.; Handa, M. *Chem. Lett.* **2002**, 1044.
(28) Liao, Y.; Shum, W. W.; Miller, J. S. *J. Am. Chem. Soc.* **2002**, *124*, 9336.
(29) Vos, T. E.; Liao, Y.; Shum, W. W.; Her, J.-H.; Stephens, P. W.; Reiff, W. M.; Miller, J. S. *J. Am. Chem. Soc.* **2004**, *126*, 11630.
(30) Vos, T. E.; Miller, J. S. *Angew. Chem., Int. Ed.* **2005**, *44*, 2416.
(31) Wang, S.; Zuo, J. L.; Zhou, H. C.; Choi, H. J.; Ke, Y. X.; Long, J. R.; You, X. Z. *Angew. Chem., Int. Ed.* **2004**, *43*, 5940.
(32) Wang, C. F.; Zuo, J. L.; Bartlett, B. M.; Song, Y.; Long, J. R.; You, X. Z. *J. Am. Chem. Soc.* **2006**, *128*, 7162.
(33) Liu, W.; Wang, C. F.; Li, Y. Z.; Zuo, J. L.; You, X. Z. *Inorg. Chem.* **2006**, *45*, 10058.
(34) Wang, S.; Zuo, J. L.; Gao, S.; Song, Y.; Zhou, H. C.; Zhang, Y. Z.; You, X. Z. *J. Am. Chem. Soc.* **2004**, *126*, 8900.
(35) Wen, H. R.; Wang, C. F.; Song, Y.; Gao, S.; Zuo, J. L.; You, X. Z. *Inorg. Chem.* **2006**, *45*, 8942.
(36) Lescouezec, R.; Toma, L. M.; Vaissermann, J.; Verdaguer, M.; Delgado, F. S.; Ruiz-Perez, C.; Lloret, F.; Julve, M. *Coord. Chem. Rev.* **2005**, *249*, 2691.
(37) Yang, J. Y.; Shores, M. P.; Sokol, J. J.; Long, J. R. *Inorg. Chem.* **2003**, *42*, 1403.
(38) Li, D. F.; Parkin, S.; Wang, G. B.; Yee, G. T.; Clerac, R.; Wernsdorfer, W.; Holmes, S. M. *J. Am. Chem. Soc.* **2006**, *128*, 4214.
(39) Gu, Z. G.; Liu, W.; Yang, Q. F.; Zhou, X. H.; Zuo, J. L.; You, X. Z. *Inorg. Chem.* **2007**, *46*, 3236.
(40) Lescouezec, R.; Vaissermann, J.; Lloret, F.; Julve, M.; Verdaguer, M. *Inorg. Chem.* **2002**, *41*, 5943.
(41) Wang, C. F.; Liu, W.; Song, Y.; Zhou, X. H.; Zuo, J. L.; You, X. Z. *Eur. J. Inorg. Chem.* **2008**, 717.
(42) Xu, G.-L.; Jablonski, C. G.; Ren, T. *Inorg. Chim. Acta* **2003**, *343*, 387.

Table 1. Crystal Data for Compounds **1**−**4**

	1·3H_2O	**2**·6H_2O·3CH_3CN	**3**·H_2O·4CH_3CN	**4**·8H_2O
formula	$C_{60}H_{70}B_2Fe_2N_{26}O_3Ru_2$	$C_{68}H_{89}B_2Fe_2N_{29}O_6Ru_2$	$C_{76}H_{94}B_2Fe_2N_{30}ORu_2$	$C_{72}H_{88}B_2Fe_2N_{26}O_8Ru_2$
fw	1538.88	1744.14	1779.27	1781.14
space group	$P\bar{1}$	*C2/c*	$P\bar{1}$	$P\bar{1}$
a, Å	10.3051(18)	35.403(9)	12.9801(18)	12.8423(18)
b, Å	13.592(2)	19.887(5)	18.403(3)	14.030(2)
c, Å	14.5407(16)	13.048(3)	19.2234(14)	24.2431(13)
α, deg	84.427(2)°	90	79.267(2)	90.287(2)
β, deg	83.004(4)	100.331(4)	78.529(3)	95.527(3)
γ, deg	72.043(3)	90	78.887(2)	92.5110(10)
V, Å3	1919.2(5)	9038(4)	4363.3(10)	4343.4(9)
Z	1	4	2	2
T, K	291(2)	291(2)	291(2)	291(2)
σ_{calcd}, g cm^{-3}	1.332	1.282	1.354	1.362
μ (mm^{-1})	0.814	0.703	0.725	0.733
GOF on F^2	1.097	1.076	1.043	1.003
R_1,[a] wR_2[b] ($I > 2\sigma(I)$)	0.066, 0.134	0.045, 0.097	0.060, 0.117	0.054, 0.113

[a] $R_1 = \sum||C|| - ||F_c||/\sum F_o||$. [b] $R_2 = [\sum w(F_o^2 - F_c^2)^2/\sum w(F_o^2)]^{1/2}$.

weeks. Yield: 54%. Anal. calcd for $C_{76}H_{94}B_2Fe_2N_{30}ORu_2$ (%): C, 51.30; H, 5.32; N, 23.62. Found: C, 51.45; H, 5.06; N, 23.40. IR (KBr, cm^{-1}): 2129 (ν_{CN}).

[(PhTp)Fe(CN)$_3$]$_2$[Ru$_2$(DMBA)$_4$] (4). A mixture of acetonitrile and water (v/v 4:1, 12 mL) was gently layered on top of a solution of $Ru_2(DMBA)_4(NO_3)_2$ (14 mg, 0.015 mmol) in 4 mL of acetonitrile and water (v/v 2:1); then, a solution of $(Bu_4N)[(PhTp)Fe(CN)_3]$ (21 mg, 0.030 mmol) in 2 mL of acetonitrile was added carefully as a third layer. Dark green needlelike crystals of **4** were obtained after one month. Yield: 47%. Anal. calcd for $C_{72}H_{88}B_2Fe_2N_{26}O_8Ru_2$ (%): C, 48.55; H, 4.98; N, 20.45. Found: C, 48.79; H, 4.97; N, 20.18. IR (KBr, cm^{-1}): 2132 (ν_{CN}).

X-Ray Crystallography. The crystal structures of compounds **1**−**4** were determined on a Siemens (Bruker) SMART CCD diffractometer using monochromated Mo Kα radiation ($\lambda = 0.71073$ Å) at room temperature. Cell parameters were retrieved using SMART software and refined using SAINT[43] on all observed reflections. Data were collected using a narrow-frame method with scan widths of 0.30° in ω and an exposure time of 10 s/frame. The highly redundant data sets were reduced using SAINT[43] and corrected for Lorentz and polarization effects. Absorption corrections were applied using SADABS[44] supplied by Bruker. Structures were solved by direct methods using the program SHELXL-97.[45] The positions of the metal atoms and their first coordination spheres were located from direct-method *E* maps; other non-hydrogen atoms were found using alternating difference Fourier syntheses and least-squared refinement cycles and, during the final cycles, were refined anisotropically. Hydrogen atoms were placed in calculated positions and refined as riding atoms with a uniform value of U_{iso}. Information concerning crystallographic data collection and structure refinement is summarized in Table 1.

Results and Discussion

Molecular Structures. Single crystal X-ray diffraction studies revealed that compounds **1**, **3**, and **4** crystallize in the triclinic $P\bar{1}$ space group, and compound **2** is in the monoclinic *C2/c* space group. The structural representations of these compounds are provided in Figure 1, while the selected geometric parameters are given in Table 2. Common to all four compounds is the $[LFe(CN)_3]^-$ complex that occupies each of the axial sites of $[Ru_2(DMBA)_4]^{2+}$ via the *N* coordination to the Ru center by a cyanide ligand. Thus, the structural study of compounds **1**−**4** confirms the formation of a "complex of complexes".

The Ru−Ru bond lengths in compounds **1**−**4** are 2.2951(8), 2.2951(6), 2.3043(6), and 2.2954(4) Å, respectively, which are slightly elongated from that in $Ru_2(DMBA)_4(NO_3)_2$ (2.2865(4) Å)[42] but almost identical to that in $Ru_2(DMBA)_4(NC-N-CN)_2$ (2.308(1) Å) and both compounds of a triply bonded Ru_2 center.[46] These bond lengths are significantly shorter than that in $Ru_2(DMBA)_4(CN)_2$ (2.4508(9) Å),[46] which contains a Ru−Ru single bond. On the basis of structural data, it is clear that the Ru_2 centers in compounds **1**−**4** are triply bonded.

In compounds **1**−**4**, each of the Ru^{3+} ions is in an axially elongated octahedral geometry. The $Ru-N_{ax}$ bond lengths are 2.343(4) Å (**1**), 2.298(3) Å (**2**), 2.257(4) and 2.307(4) Å (**3**), and 2.221(3) and 2.357(3) Å (**4**), which are about the same as the $Ru-N_{ax}$ bond length in $Ru_2(DMBA)_4(NC-N-CN)_2$ (2.28(1) Å), but much larger than the $Ru-C_{ax}$ bond length in $Ru_2(DMBA)_4(CN)_2$ (1.983(5) Å). The structural data are consistent with a weak $N_{ax} \rightarrow$ Ru dative bond in compounds **1**−**4**, which is corroborated by the insignificant shift of ν(C≡N) observed for **1**−**4** in comparison with that of $(Bu_4N)[(L)Fe(CN)_3]$. The $Ru-Ru-N_{ax}$ (177.29(10)−179.59(10)°) bond angles are quite close to linearity. Four nitrogen atoms from the DMBA ligands form the equatorial plane with nearly equal $Ru-N_{eq}$ bond lengths, and the $Ru-Ru-N_{eq}$ bond angles are close to 90°. Therefore, the coordination sphere of the Ru_2 core in **1**−**4** is of approximate D_{4h} symmetry. Each octahedral $[(L)Fe(CN)_3]^-$ unit uses one of three cyanide ligands to connect the $[Ru_2(DMBA)_4]^{2+}$ ion, which results in a long Fe−C≡N−Ru−Ru−N≡C−Fe chain with Fe−C≡N and Ru−N≡C angles falling in the range 170.1(3)−177.7(4)°. The Fe−C bond distances (1.863(5)−1.944(5) Å) are comparable to those observed previously for structures containing $[LFe(CN)_3]^-$.[31−35,38−40] The intramolecular Fe···Fe

(43) *SAINT-plus*, version 6.02; Bruker Analytical X-ray System: Madison, WI, 1999.
(44) Sheldrick, G. M. *SADABS*; Bruker Analytical X-ray System: Madison, WI, 1996.
(45) Sheldrick, G. M. *SHELXL-97*; University of Göttigen: Göttigen, Germany, 1997.
(46) Chen, W.-Z.; Ren, T. *Inorg. Chem.* **2003**, *42*, 8847.

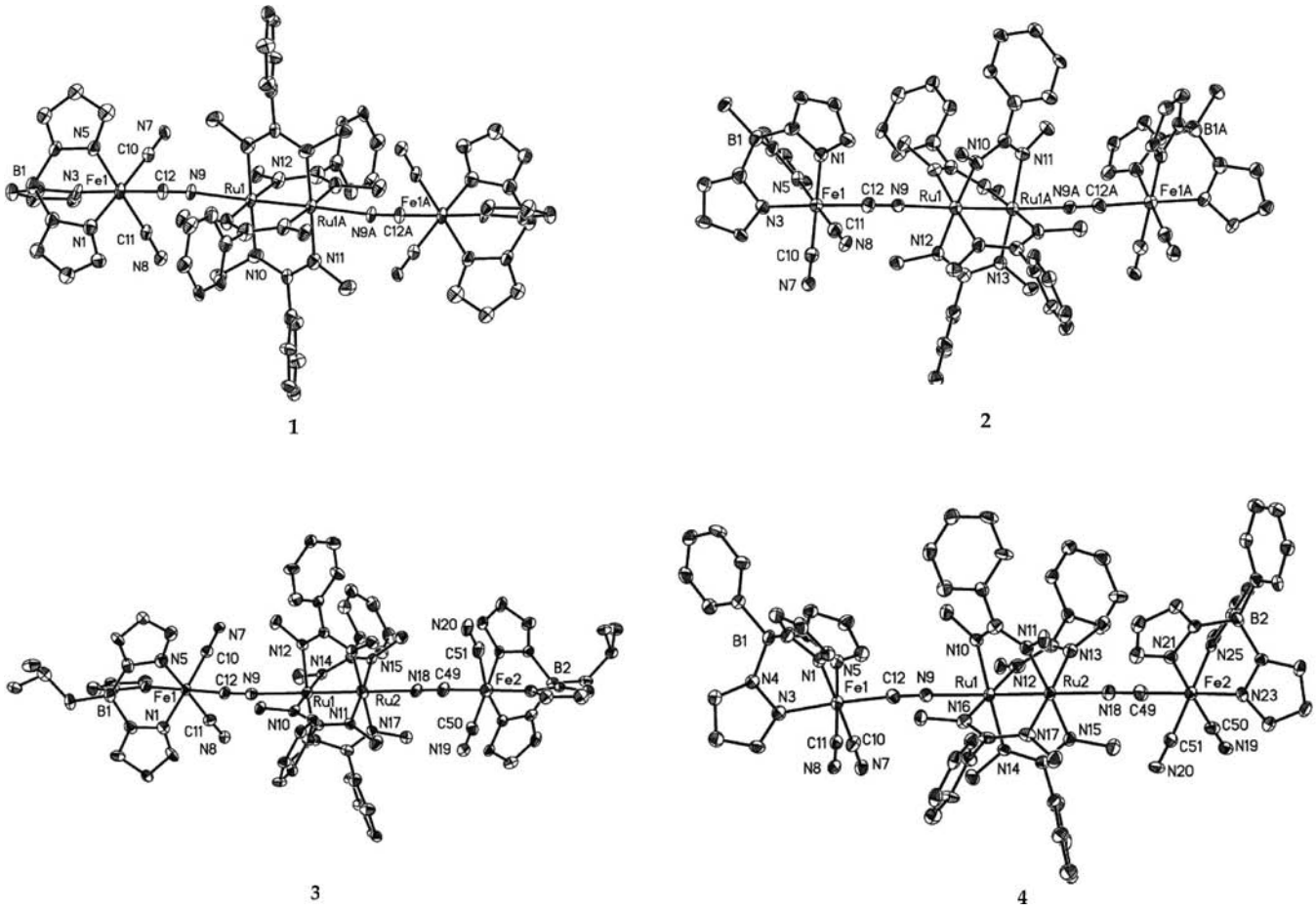

Figure 1. ORTEP plots of compounds **1**−**4** at the 30% probability level. Hydrogen atoms are omitted for clarity.

Table 2. Selected Bond Lengths (Å) and Angles (deg) for Compounds **1**−**4**

	1	**2**		**3**	**4**		**3**	**4**
Ru1−Ru1^a	2.2951(8)	2.2951(6)	Ru1−Ru2	2.3043(6)	2.2954(4)	Fe1−C12	1.890(4)	1.905(4)
Ru1−N9	2.343(4)	2.298(3)	Ru1−N9	2.307(4)	2.357(3)	Fe2−C49	1.863(5)	1.885(4)
Ru1−N10	2.026(5)	2.039(2)	Ru2−N18	2.257(4)	2.221(3)	Fe2−C50	1.944(5)	1.928(4)
Ru1−N11^a	2.050(5)	2.049(2)	Ru1−N10	2.033(3)	2.009(3)	Fe2−C51	1.922(5)	1.913(4)
Ru1−N12	2.036(4)	2.036(2)	Ru1−N12	2.036(3)	2.048(3)			
Ru1−N13^a	2.028(5)	2.011(2)	Ru1−N14	2.050(3)	2.013(3)	Fe1−C12−N9	170.2(4)	172.9(4)
Fe1−N1	1.960(5)	1.967(3)	Ru1−N16	2.055(3)	2.026(3)	C12−N9−Ru1	170.1(3)	170.3(3)
Fe1−N3	1.924(4)	1.973(2)	Ru2−N11	2.066(3)	2.063(4)	N9−Ru1−Ru2	178.78(9)	178.33(9)
Fe1−N5	1.965(5)	1.976(2)	Ru2−N13	2.051(4)	2.024(3)	Ru1−Ru2−N18	178.77(9)	179.59(10)
Fe1−C10	1.916(6)	1.924(3)	Ru2−N15	2.046(3)	2.029(3)	Ru2−N18−C49	174.5(2)	176.7(4)
Fe1−C11	1.904(5)	1.918(3)	Ru2−N17	2.058(3)	2.035(3)	N18−C49−Fe2	177.5(4)	177.7(4)
Fe1−C12	1.869(5)	1.902(3)	Fe1−N1	1.961(4)	1.956(4)	N10−Ru1−Ru2	88.83(10)	89.01(9)
Fe1−C12−N9	172.5(5)	174.6(3)	Fe1−N3	2.013(3)	1.980(3)	N12−Ru1−Ru2	88.28(9)	88.75(10)
C12−N9−Ru1	173.3(4)	174.7(3)	Fe1−N5	1.956(4)	1.952(3)	N14−Ru1−Ru2	89.25(9)	88.80(9)
N9−Ru1−Ru1^a	177.29(11)	178.08(6)	Fe2−N21	1.960(4)	1.957(3)	N16−Ru1−Ru2	89.34(9)	88.07(10)
N10−Ru1−Ru1^a	88.97(13)	88.32(7)	Fe2−N23	1.882(4)	1.934(3)	Ru1−Ru2−N11	88.96(9)	88.18(9)
N11^a−Ru1−Ru1^a	88.13(12)	88.09(7)	Fe2−N25	1.932(4)	1.972(3)	Ru1−Ru2−N13	89.45(10)	89.26(9)
N12−Ru1−Ru1^a	88.49(12)	87.73(6)	Fe1−C10	1.918(4)	1.902(4)	Ru1−Ru2−N15	87.73(9)	88.39(9)
N13^a−Ru1−Ru1^a	88.41(12)	89.50(7)	Fe1−C11	1.944(5)	1.915(4)	Ru1−Ru2−N17	88.76(9)	89.52(10)

^{a} Symmetry transformation used to generate equivalent atoms: $-x + 1, -y + 1, -z + 1$ for **1** and $-x, y, -z + 1/2$ for **2**.

separations in **1**− **4** are 12.929, 12.908, 12.891, and 12.901 Å, respectively.

Magnetic Properties. Magnetic measurements were performed on polycrystalline samples of $Ru_2(DMBA)_4(NO_3)_2$ and compounds **1**−**4**. As shown in Figure 2, the value of $\chi_M T$ (μ) for $Ru_2(DMBA)_4(NO_3)_2$ at 300 K is 1.14 emu K mol^{-1} (3.0 μ_B), which is in good agreement with an $S = 1$ ground state ($\mu = g\sqrt{S(S+1)}\mu_B = 2.8\ \mu_B$) . As the temperature decreases, the $\chi_M T$ value decreases slowly and reaches 0.017 emu K mol^{-1} at 1.8 K, which is primarily due to the zero-field splitting (ZFS) of the $^3A_{2g}$ ground state, leading to the only population on the $M_S = 0$ state.[47,48] This conclusion is confirmed by the very small value of field-

(47) Cotton, F. A.; Miskowski, V. M.; Zhong, B. *J. Am. Chem. Soc.* **1989**, *111*, 6177.
(48) Cotton, F. A.; Ren, T.; Wagner, M. J. *Inorg. Chem.* **1993**, *32*, 965.

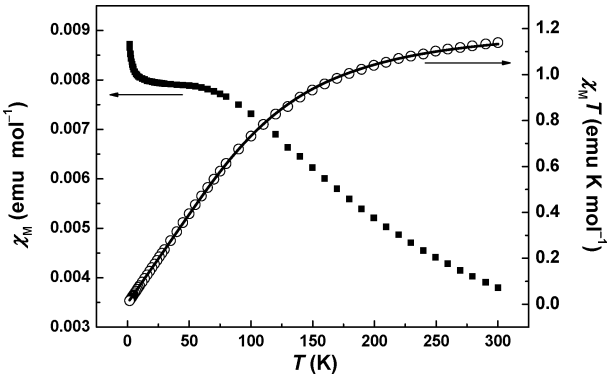

Figure 2. The temperature dependence of χ_M (square) and $\chi_M T$ (circle) for $Ru_2(DMBA)_4(NO_3)_2$ recorded under a 2 kOe field. The solid line represents the fitting to the data.

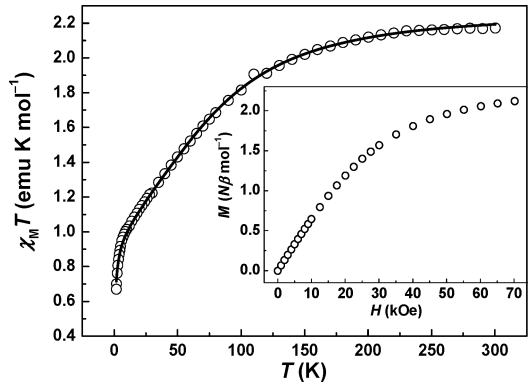

Figure 3. The temperature dependence of $\chi_M T$ for compound **2** under 2 kOe. The solid line represents the best fit. Inset: Field dependence of magnetization for **2** measured at 1.8 K.

dependent magnetization at 1.8 K (Figure S1, Supporting Information). The temperature dependence of magnetic susceptibility can be quantified using eq 1[47,48]

$$\chi = \frac{2Ng^2\beta^2}{3kT} \times \frac{e^{-x} + \frac{2}{x}(1 - e^{-x})}{1 + 2e^{-x}} \quad (1)$$

where $x = D/kT$ and D is the ZFS parameter. The abrupt increase of χ_M at very low temperatures could be attributed to a small amount of paramagnetic impurity (possibly a $Ru_2^{II,III}$ species). This effect is taken into account by eq 2

$$\chi_M = (1 - \rho)\chi + \rho\frac{5Ng_{imp}^2\beta^2}{4kT} \quad (2)$$

where ρ is the molar fraction of paramagnetic impurity and the value of g_{imp} is assumed to be 2.0 by convention. Least-squares fitting of the $\chi_M T$ data in the whole temperature range gave $g = 2.200$, $D = 216.45$ cm^{-1}, and $\rho = 0.2\%$ with $R = \sum[(\chi_M T)_{calcd} - (\chi_M T)_{obsd}]^2/\sum(\chi_M T)^2_{obsd} = 8.2 \times 10^{-6}$. The temperature-dependence of magnetic susceptibility of $Ru_2(DMBA)_4(NO_3)_2$ is quite similar to those previously observed for Os_2^{6+}, Ru_2^{4+}, and Ru_2^{6+} compounds with an $^3A_{2g}$ ground state, and the ZFS parameter (D) is very close to those of comparable Ru_2(III) species, namely, $Ru_2(hpp)_4Cl_2$ ($D = 227$ cm^{-1}) and $Ru_2(hpp)_4(SO_3CF_3)_2$ ($D = 243$ cm^{-1}).[47−51]

As shown in Figure 3 and Figures S2−S4 (Supporting Information), compounds **1**−**4** display very similar magnetic behavior. Upon lowering the temperature, the $\chi_M T$ values decrease continuously from the room temperature values of 2.12 (**1**), 2.17 (**2**), 2.28 (**3**), and 2.16 (**4**) emu K mol^{-1} and reach 1.0 (**1**), 0.95 (**2**), and 0.97 (**3** and **4**) emu K mol^{-1} at 6 K (**1** and **2**) and 4 K (**3** and **4**). The change observed ($\Delta(\chi_M T)$), *ca.* −1.2 emu K mol^{-1}, is about the same as that observed for $Ru_2(DMBA)_4(NO_3)_2$ over the same temperature window and, hence, is mainly attributed to the zero-field splitting at the Ru_2 center, while the magnetic interaction between the iron and Ru_2 center is weak. At lower temperatures, the susceptibilities drop down sharply and reach the minimum values of 0.783 (**1**), 0.67 (**2**), 0.86 (**3**), and 0.90 (**4**) emu K mol^{-1} at 1.8 K, which indicates a very weak antiferromagnetic (AF) interaction between two $[(Tp-)Fe(CN)_3]^-$ ($S = 1/2$) units (Figure S5, Supporting Information). Weak intra- and intermolecular antiferromagnetic interactions between the low-spin iron(III) ($S = 1/2$) centers may account for this decrease. In addition, the field-dependent magnetization shows a value of 1.88 (**1**) under 5 T and 2.12(**2**), 2.19 (**3**), and 2.30 (**4**) $N\beta$ mol^{-1} under 7 T at 1.8 K (the inset in Figure 3 and Figures S2−S4, Supporting Information), comparable to the expected spontaneous magnetization for two low-spin Fe^{III} ($S = 1/2$) ions. It further confirms the ZFS effect at the Ru_2 centers, which are trended to be nonmagnetic at very low temperatures.

In an attempt to further quantify the weak interaction in compounds **1**−**4**, an approximate model treating the AF coupling as a perturbation to the ZFS was expressed in the following equations:

$$\chi = \chi_{Ru2} + 2\chi_{Fe} = \frac{2Ng^2\beta^2}{3kT}\frac{e^{-x} + \frac{2}{x}(1 - e^{-x})}{1 + 2e^{-x}} + \frac{2Ng^2\beta^2}{3kT}S_{Fe}(S_{Fe} + 1) \quad (3)$$

$$\chi_M = \frac{\chi}{1 - (2zj'/Ng^2\beta^2)\chi} \quad (4)$$

where $x = D/kT$ and zj' represents the antiferromagnetic coupling either between the Fe centers. The least-squares fittings of the $\chi_M T$ data according to eqs 3 and 4 revealed good agreement between the model and experimental data, and the result for compound **2** is shown in Figure 3. The parameters g, D/cm^{-1}, and zj'/cm^{-1} derived from the least-squares fittings are 2.234, 168.29, and −0.031 ($R = 3.6 \times 10^{-3}$) for **1**; 2.275, 183.34, and −0.468 ($R = 2.1 \times 10^{-4}$) for **2**; 2.326, 212.27, and −0.233 ($R = 4.0 \times 10^{-5}$) for **3**; and 2.256, 191.36, and −0.063 ($R = 1.0 \times 10^{-4}$) for **4**.

Spectroscopic Properties. Both the FT-IR and vis−NIR spectroscopic properties of compounds **1**−**4** were investigated. The C≡N stretches in compounds **1**−**4** were observed at 2127, 2124, 2129 and 2132 cm^{-1}, respectively, while those of the corresponding $[(L)Fe(CN)_3]^-$ precursors were observed

(49) Cotton, F. A.; Murillo, C. A.; Reibenspies, J. H.; Villagrán, D.; Wang, X.; Wilkinson, C. C. *Inorg. Chem.* **2004**, *43*, 8373.
(50) Bear, J. L.; Li, Y.; Han, B.; Kadish, K. M. *Inorg. Chem.* **1996**, *35*, 1395.
(51) Miskowski, V. M.; Gray, H. B. *Topics Cur. Chem.* **1997**, *191*, 41.

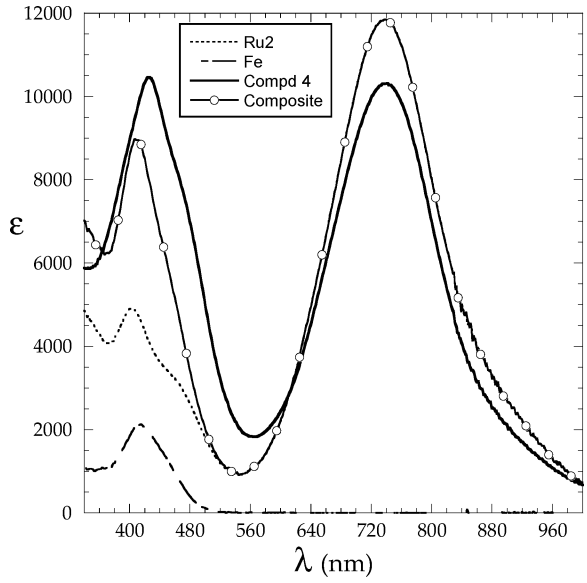

Figure 4. Vis−NIR spectra of compound **4**, $Ru_2(DMBA)_4(NO_3)_2$ ("Ru2"), and $[(PhTp)Fe(CN)_3]^-$ ("Fe") recorded in CH_2Cl_2. Also shown is a composite spectrum from summing that of "Ru2" and twice of "Fe".

at 2117, 2120, 2117, and 2119 cm^{-1}, respectively.[41] The minimal shift in $\nu(C\equiv N)$ is indicative of the absence of $Ru-N_{ax}$ π-backbonding in compounds **1**−**4**.

The Vis-NIR spectra of compounds **1**−**4** recorded in CH_2Cl_2 are very similar, and the spectrum of **4** is shown in Figure 4 along with those of the Ru_2 precursor, $Ru_2(DMBA)_4(NO_3)_2$, and the Fe precursor, $(Bu_4N)[(PhTp)Fe(CN)_3]$, while those of compounds **1**−**3** can be found in Figure S6 in the Supporting Information. Compound **4** exhibits two equally intense peaks at 425 and 741 nm, and a shoulder around 470 nm. The peak at 741 nm is clearly originated from the Ru_2 moiety since (i) $Ru_2(DMBA)_4(NO_3)_2$ absorbs intensely in this region (λ_{max} = 738 nm) and (ii) $[(PhTp)Fe(CN)_3]^-$ does not absorb in this region at all. The peak at 425 nm arises from the contributions of both $[(PhTp)Fe(CN)_3]^-$ and $Ru_2(DMBA)_4(NO_3)_2$, which have bands of medium intensity at 412 and 401 nm, respectively. Also shown in Figure 4 is a "composite spectrum" constructed from the sum of the $Ru_2(DMBA)_4(NO_3)_2$ spectrum and twice of the $[(PhTp)Fe(CN)_3]^-$ spectrum. Since the composite spectrum closely tracks that of **4**, the Ru_2 and Fe chromophores are fairly independent of each other in **4**. This observation is consistent with the absence of significant *intermetallic* electronic coupling concluded from the magnetic studies.

Electrochemical Properties. Diruthenium species are known to exhibit rich redox activity, and compounds **1**−**4** are no exception.[5,52] The cyclic voltammograms (CVs) were recorded in CH_2Cl_2, and the CV for compound **1** is given in Figure 5. Compounds **1**−**4** all display two quasi-reversible one-electron reductions: the first at *ca.* −0.81 V (**A**) and the second at *ca.* −1.07 V (**B**). Assignment of these couples is challenging due to the coexistence of three redox centers. Hence, the CVs of $Ru_2(DMBA)(NO_3)_2$ ("Ru_2") and $(Bu_4N)[(Tp)Fe(CN)_3]$ ("Fe") recorded in CH_2Cl_2 were also included in Figure 5 for comparison. The CV of $Ru_2(DMBA)(NO_3)_2$ features a quasi-reversible

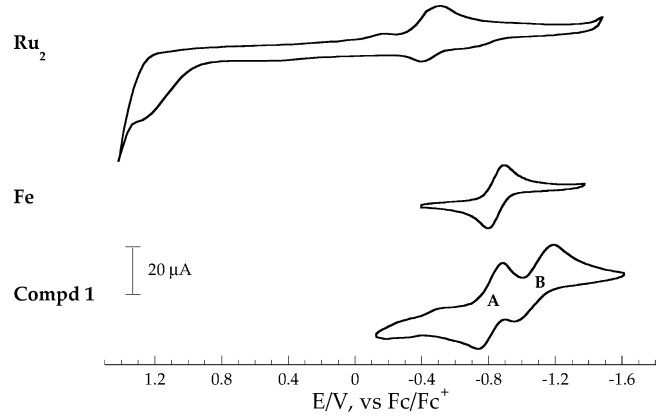

Figure 5. Cyclic voltammograms of compound **1**, $Ru_2(DMBA)(NO_3)_2$ (Ru_2), and $(Bu_4N)[(Tp)Fe(CN)_3]$ (Fe) recorded in CH_2Cl_2 with scan rate of 100 mV/s.

one-electron reduction at −0.48 V and an irreversible oxidation at *ca.* 1.1 V, while that of $(Bu_4N)[(Tp)Fe(CN)_3]$ features a reversible one-electron reduction at −0.84 V. A plausible assignment of the couples observed for **1** is that couple **A** is Ru_2-based and **B** is Fe-based. The cathodic shift of $E_{1/2}$(**A**) from that of $Ru_2(DMBA)(NO_3)_2$ is attributed to the fact that $[(Tp)Fe(CN)_3]^-$ is a better donor than NO_3^-. It seems odd that there is only one $1e^-$ wave of Fe (**B**) detected instead of either a $2e^-$ wave or a pair of $1e^-$ waves. This is likely due to an electrostatic effect: the existence of a negative charge on the central Ru_2 unit makes the simultaneous reduction of both Fe centers thermodynamically unfavorable. Upon the completion of reduction **B**, the complex becomes a dianion ($[\mathbf{1}]^{2-}$), and the potential required to further reduce $[\mathbf{1}]^{2-}$ is probably beyond the potential window permitted by the solvent. Overall, the redox behaviors of compounds **1**−**4** are sluggish compared with those of $Ru_2(DMBA)_4(C_2R)_2$-type compounds,[53−55] which are caused by ready cleavage of the weak Ru−N≡C dative bond in the former compounds under electrochemical conditions. Closer examination of the CV of **1** also revealed a small "hump" at *ca* −0.40 V, which could be originated from a Ru_2−Fe species generated *in situ* from the cleavage of one of the Ru−N≡C bonds in **1**. Such behaviors have been frequently observed in diruthenium species of weakly coordinated axial ligands.[46]

Conclusion

We have prepared a family of heterometallic compounds **1**−**4** from the combination of $Ru_2(DMBA)_4(NO_3)_2$ and $[LFe(CN)_3]^-$ synthons. The structural, magnetic, spectroscopic, and electrochemical studies all indicate the modular nature of these species: namely, that the covalently linked Fe and Ru_2 centers remain electronically independent of each other. It is possible that linkages via stronger bonds are needed to elicit significant *intermetallic* interactions within

(52) Ren, T.; Xu, G.-L. *Comm. Inorg. Chem.* **2002**, *23*, 355.
(53) Xu, G.-L.; Campana, C.; Ren, T. *Inorg. Chem.* **2002**, *41*, 3521.
(54) Xu, G.-L.; DeRosa, M. C.; Crutchley, R. J.; Ren, T. *J. Am. Chem. Soc.* **2004**, *126*, 3728.
(55) Xu, G.-L.; Crutchley, R. J.; DeRosa, M. C.; Pan, Q.-J.; Zhang, H.-X.; Wang, X.; Ren, T. *J. Am. Chem. Soc.* **2005**, *127*, 13354.

a "complex of complexes", which is currently under investigation in our laboratories.

Acknowledgment. This work was supported in part by the National Natural Science Foundation of China (Grant Nos. 20531040 and 20725104), the "111 Project" of the Ministry of Education of China, and the U.S. National Science Foundation (Grants No. CHE 0715404). We thank a reviewer for invaluable comments on both the modeling of magnetic data and structural refinements, and Prof. Yi-Zhi Li for his assistance on crystallographic work.

Supporting Information Available: Field dependence of magnetization for $Ru_2(DMBA)_4(NO_3)_2$ and compounds **1**−**4** at 1.8 K, visible−NIR spectra of compounds **1**−**3**, and X-ray crystallographic files in CIF format for compounds **1**, **2**, **3**, and **4.** This material is available free of charge *via* the Internet at http://pubs.acs.org.

IC8011684